A Network SIR Model of Epidemics: Evidence for the United States and Brazil

Keven Roger Alves André* **Marcelo Arbex‡** **Márcio V. Corrêa†**

August 2, 2022

Abstract

We study how a network structure can determine the evolution of an epidemic. For that, we use a Susceptible-Infected-Recovered (SIR) macroeconomic model in the presence of a network environment. Network models have been important in the job search discussion. In an epidemiological model, the network structure is one of the main causes of the spread of the disease. Intuitively, more connected people in the social circle are the main vector of the virus. On the other hand, those people with few connections should be less exposed to the disease. We study the behavior of the pandemic for different types of network, from a low connected one to a high connected one. We find exactly the expected relationship: because more connected economies (economies with a higher average number of links) spread the virus faster, they face harder consequences in a pandemic scenario, such as a greater fall on aggregate consumption and hours worked due to both the higher number of deaths and the susceptible agents' higher attempt to stay at home and avoid physical contacts. Susceptible agents are more cautious in regard to the decision of their level of consumption and hours worked as the economy becomes more socially connected, once the consequences of leaving home to consume or to work are harder in the higher connected economy because of its higher number of infected people.

Keywords: Pandemic; Epidemiological model; Networks

JEL Classification: D85, I10

*CAEN - Graduate Studies in Economics, Federal University of Ceará, Brazil. Email: kevenroger319@gmail.com. ‡Department of Economics, University of Windsor, Canada. CAEN/UFC International Visiting Professor. E-mail: arbex@uwindsor.ca; †CAEN - Graduate Studies in Economics, Federal University of Ceará, Brazil. Email: marciovcorrea@caen.ufc.br

1 Introduction

In this paper, we extend the SIR-macro model proposed by Eichenbaum et al. (2020) to study the implications and the role of the social network on the evolution of a pandemic. Exploring the role of the social network in the behavior of the pandemic is quite important for the choice of policy measures to contain the spread of the virus. In fact, adopting a network perspective provides insights that can enrich the analysis of the economic implications of a pandemic. For example, in the Network SIR-Macro model proposed significant heterogeneity in connections can accelerate the early spread of disease while reducing the share of the population that is affected in the long run. This result affects the relative benefits of lockdown policies in models that trade off economic disruption for a slowdown in the spread of the disease, such as in (Eichenbaum et al., 2020).

Allowing for heterogeneity in economic analyses of the disease's impact can provide substantial benefits, as different groups might contribute differently to economic output as they do for disease outcomes (Acemoglu et al., 2021). Our main contribution is to incorporate irregular networks into a SIR-model of infectious disease. In particular, by acknowledging the role of heterogeneity in network connections, we provide one reason that agents are not equally likely to receive the virus through their links. This article provides a framework to analyze the dynamics of the epidemic and the optimal behaviour of the economic agents as driven by (non-observable) agent heterogeneity in social connections.

The COVID-19 pandemic represents the worst economic crisis since the Great Depression (Gopinath (2020)). Given the rapid spread of COVID-19, countries across the World have adopted several public health measures intended to prevent its spread, including social distancing. A contact network plays a key role at the dynamics of infectious diseases and other transmission phenomena. Despite the uniqueness of the virus, the macroeconomics of an epidemic depends on local characteristics. Our main contribution to the discussion of the macroeconomics of epidemics is the implications of the social network on the spread of the virus. In particular, we simulate the model for different social networks from a less connected one to a more connected network. Results show that the economies that present more connections in the social network face a more severe

pandemic, measured by the number deaths and the drop in consumption and output. People's decisions to cut back on consumption and work reduce the severity of the pandemic. These same decisions exacerbate the size of the recession caused by the pandemic (Brinca et al., 2021).

The SIR model is a model widely used by epidemiologists, and was initially developed by Kermack and McKendrick (1927). It proposes three health status: susceptible, infected and recovered. Susceptible people can contract the virus through interaction with the infected ones. Infected people can transmit the virus, and also can either dye or recover. Recovered people are immune and can no longer transmit the virus. The infection, recovery and mortality rate are the main parameter of such model. A feature of epidemiological models is that the transitions between the health status are exogenous with respect to the economic variables. In other words, the expected fall on consumption and hours worked are not considered in the SIR models.[1]

In Eichenbaum et al. (2020)'s SIR-macro model, the number of infections depends on the level of interaction between the agents when they consume and work, and on other residual ways of infection. Therefore the susceptible population can reduce the odds of infection by reducing their consumption level and hours worked. The competitive equilibrium, however, is not Pareto efficient, for the infected and recovered agents do not take into account that their actions influence the other agents' infection and mortality rates. Bethune and Korinek (2020) focus on this type of externality. The authors develop Susceptible-Infected-Susceptible (SIS) and SIR models to quantify the externalities of infection using both decentralized and social planner approaches. They find that, in a decentralized approach, the infected agents keep engaged in economics activities in order to maximize utility, while the susceptible agents reduce their activities to reduce the odds of infection. With a social planner approach, the planner forcefully reduces the infected agents' activities to mitigate the risk of the susceptible agents. In our model, this externality has its impact amplified (reduced) by the agents' degree of socialization. The greater the number of peers of an infected agent, the greater the externality caused in susceptible individuals. Thus, if the social planner imposed containment measures for infected agents, with the aim of reducing transmission rates, those with a greater number of peers would suffer a greater level of social exclusion.

Berger et al. (2020) study this incomplete information using a Susceptible-Exposed-Infected-

[1]For a complete literature review of the economics of COVID-19, see Brodeur et al. (2021).

Recovered (SEIR) model based on Kermack and McKendrick (1927). They work on the idea of increasing the tests in the susceptible population to identify asymptomatic infected patients looking to isolated that part of the population. The authors find that such directed quarantine policy softens the negative impact of the pandemic on the economy and reduces the peak of infection. Some countries adopted the vertical isolation for the risk group. Acemoglu et al. (2020) study this question with a multi-risk SIR model (MR-SIR) and divide the population in different groups (young, middle-aged and old), with different infection, hospitalization and mortality rates. Those conditions allow the possibility of vertical quarantine policy. The heterogeneous lockdown across different groups, been more severe for the higher risk group (the old), can reduce both the number of lives lost and the economic recession when compared with horizontal lockdowns.

With respect to the Brazilian economy, Rabelo and Soares (2020) exploit the model proposed by Eichenbaum et al. (2020) calibrating the parameters with Brazilian data. They found that an optimal social containment policy causes a larger recession in the short run than in the case where no measure of social containment are taken. On the other hand, the optimal containment policy has the ability to save about 50 thousand lives. Borelli and Góes (2020) uses the same model study the implications of COVID-19 on the states of São Paulo, Amazonas, Ceará, Rio de Janeiro and Pernambuco. Results point to great heterogeneity, which suggests that each state may require specific measures. São Paulo is the state whose infected population reaches the higher fraction of its total population in the competitive equilibrium between those five states studied. Meanwhile, the macroeconomic shocks are more severe at Ceará and Pernambuco.

Besides this introduction, this paper is organized in X additional sections. Section 2 presents the Network SIR-Macro Model. A quantitative analysis and results for the United States are presented in Section 3. In Section 4 an application to the Brazilian Economy is presented and discussed. Section 5 concludes.

2 A Network SIR-Macro Model

Epidemiology models generally assume that the probabilities governing the transition between different states of health are exogenous with respect to economic decisions. Eichenbaum et al.

(2020) modify the canonical SIR model proposed by Kermack and McKendrick (1927) so that these transition probabilities depend on people's economic decisions. Since purchasing consumption goods or working brings people into contact with each other, we assume that the probability of becoming infected depends on these activities. We embed a social network model along the lines of models of the transmission of information in large, complex networks (Arbex et al., 2019) (Calvo-Armengol and Jackson, 2004). This is meant to capture the fact that the probability of becoming infected depends not only on the individual's consumption and work decisions but also on the number of people he interacts with during these activities.

In this section, we describe the economy before the start of the epidemic. Next, we present the economy's demography, network structure and infection transmission through the network. We then present the SIR-macro network model.

2.1 The pre-infection economy

We present the pre-infection economy as in Eichenbaum et al. (2020) for completeness. We assume that the economy is populated by a continuum of ex-ante identical agents with measure one. Prior to the start of the epidemic, all agents are identical and maximize the objective function:

$$U = \sum_{t=0}^{\infty} \beta^t u\left(c_t, n_t\right) = \beta^t \left(\ln c_t - \frac{\theta}{2} n_t^2\right). \tag{1}$$

Here $\beta \in (0,1)$ denotes the discount factor and c_t and n_t denote consumption and hours worked, respectively. The budget constraint of the representative agent is:

$$(1+\mu_t)c_t = w_t n_t + \Gamma_t.$$

Here, w_t denotes the real wage rate, μ_t is the tax rate on consumption, and Γ_t denotes lump-sum transfers from the government. We think of μ_t as a proxy for containment measures aimed at reducing social interactions. We refer to μ_t as the containment rate. The first-order condition for the representative-agent problem is: $(1+\mu_t)\theta n_t = c_t^{-1} w_t$.

There is a continuum of competitive representative firms of unit measure that produce consumption goods (C_t) using hours worked (N_t) according to the technology: $C_t = AN_t$. The firm

chooses hours worked to maximize its time-t profits $\Pi_t = AN_t - w_t N_t$. The government's budget constraint is given by $\mu_t c_t = \Gamma_t$. In equilibrium, $n_t = N_t$ and $c_t = C_t$.

2.2 The outbreak of an epidemic

The population is divided into four groups: susceptible (people who have not yet been exposed to the disease), infected (people who contracted the disease), recovered (people who survived the disease and acquired immunity), and deceased (people who died from the disease). The fractions of susceptible, infected, recovered and deceased individuals in the population are denoted by m_t^S, m_t^I, m_t^R, and m_t^D, respectively. The number of newly infected people is denoted by T_t.

Regarding the outbreak of an epidemic, like in Eichenbaum et al. (2020), we assume that, at time zero, a fraction ε of susceptible individuals is infected by a virus through zoonotic exposure, that is, the virus is directly transmitted from animals to humans, i.e., $m_0^I = \varepsilon$, $m_0^S = 1 - \varepsilon$. And, everybody is aware of the initial infection and understands the laws of motion governing population health dynamics.

In our model, susceptible people can become infected in two ways. First, they can meet infected people while purchasing consumption goods. Second, susceptible and infected people can meet at work. In the standard SIR model as in Eichenbaum et al. (2020), the flow from susceptible to infected is proportional to the total numbers of both the susceptible and the infected. This approach seeks to capture the idea that for a given transmissibility of a virus the likelihood of infection depends on how frequently already infected individuals interact with those who are still susceptible via their consumption and labor decisions.

The standard SIR-Macro model assumes that infections evolve as if any susceptible individual interacts with and could be infected by any infected individual across the population with equal probability. However, it is well documented that social interactions are not organized in this stylized way. Instead, individuals interact mostly within much narrower groups, shaped, for example, by family ties, work and social environments, and geography. Network models provide a route into analyzing epidemics in a way that takes these patterns of interaction into account.

2.3 Demographics, Network Structure, and Infection Transmission

Explicitly modeling interaction patterns via a network can provide a number of important insights about the spread of a disease that are not present in the baseline model. The first useful feature that can be captured by a network model is that it can accommodate differences in the number of interactions between individuals in a population. For example, some individuals may live in rural environments with relatively few contacts through their work or social life, while others live in dense urban centers, using crowded public transport, working in high-contact occupations, and interacting with many others outside of work.

The second feature that network models can capture is that social networks tend to exhibit a significant degree of overlapping relationships among groups of individuals who move in the same circles. Among coworkers in a given plant, for example, it is likely that a large share of the interactions of one worker in the workplace as well as in other social circles overlap significantly with those of another worker at the same plant.

Another, more subtle, effect of the variability in the number of contacts is that individuals are more likely to become infected if their number of interactions is higher. This greater connectedness of those who get infected then implies that they are also more likely to pass on the disease themselves. This pattern of the network can contribute to accelerating the spread of the disease in the early stages. Conversely, in later stages of a disease once many highly connected individuals have recovered, infected individuals will tend to have fewer connections and thus fewer opportunities to pass on the disease.

With these insights from a network perspective, we introduce our network approach. We assume that agents are connected to one another in a network, whose structure is exogenous. Each agent may have peers to whom she passes the virus when infected, and from whom she may receive the virus when susceptible. A network is described by a *degree distribution* $\{D_z\}_{z=1}^{\infty}$, where D_z is the proportion of agents who have $z \in [1, \infty)$ peers. The power-law network has distribution $D_z = (a-1)z^{-a}$.

The probability a given peer has s links is $\psi_s = (sD_s)/\langle z \rangle$, where $\langle z \rangle = \int_{z=1}^{\infty} (zD_z)\, dz$ is the *average degree* in the network. Note that $\psi_s \neq D_s$, i.e., the probability one of your peers has s

links is not equal to the proportion of the population that has s links. This is because agents with many peers, and a large s, are disproportionately likely to be your peers, so we must scale D_s by $s/\langle z \rangle$. This gives the probability that a peer with s links passes you the virus.

The infection rate among agents with s peers is $m^I_{s,t}$. These agents contact susceptible friends either via consumption ($x = c$) or via work ($x = n$) with probability ρ^x_t, $x = c, n$. Infected agents (I) pass the virus onto other susceptible peers (S) with probability $\varphi(x^I_t, x^S_t) = (m^S_t x^S_t + m^I_t x^I_t)^{1-\lambda_x}$, $x = \{c, n\}$, where λ_x measures the efficacy of this technology. Notice that $\varphi(x^I_t, x^S_t)$ depends on how much agents engage in a particular activity x, i.e., either consumption ($x = c$) or work ($x = n$). It also depends on the way social contact occurs (with or without face masks, for example) and on the virus transmission rate (ceteris paribus, some viruses are more contagious than others). When λ_x is close to 0, the virus is transmitted at a higher rate and requires less interaction among individuals. On the other hand, when λ_x is close to 1, transmission is more difficult and will depend more on individuals' consumption or work. Hence, the role of the λ_x in our model is to capture the joint effect of the rate of contagion of the virus per se and how social contact occurs between infected and susceptible agents, facilitating (or hindering) the transmission of the disease.

Hence, for a given agent and a given activity $x = \{c, n\}$, the probability another agent of type s is infected, meet her susceptible friends, transmits the virus, and is a peer is $m^I_{s,t}\rho^x_t\varphi(x^I_t, x^S_t)\psi_s$. Integrating over all possible s, the probability a susceptible agent is infected by a peer via an activity $x = \{c, n\}$ is therefore

$$\begin{aligned}
\Omega^x_t &= \int_{s=1}^{\infty} m^I_{s,t}\rho^x_t\varphi(x^I_t, x^S_t)\psi_s ds \\
&= \rho^x_t\varphi(x^I_t, x^S_t)\frac{1}{\langle z \rangle}\int_{s=1}^{\infty} m^I_{s,t}(sD_s)ds \\
&= m^I_t\rho^x_t\varphi(x^I_t, x^S_t), \qquad (2)
\end{aligned}$$

Hence, for an activity $x = \{c, n\}$, the probability a susceptible agent of type z receives the virus from at least one peer is $p^x_t = 1 - (1 - \Omega^x_t)^z$, and the aggregate probability susceptible agents of

different types z receive the virus is

$$P_t^x = \int_{z=1}^{\infty} p_t^x D_z dz. \tag{3}$$

Recall that, in our model, the disease is transmitted from infected agents to susceptible one when they engage in two activities, i.e., consumption and work. As discussed above, these activities occur in the context of a network. That is, the number of other agents a particular infected or susceptible agents is connected to is important to determine the degree of infection transmission and its dynamic in the economy.

The timing convention in our model is as in Eichenbaum et al. (2020). Consumption and work interactions happen in the beginning of the period (infected and susceptible people meet). Then, changes in health status unrelated to social interactions (recovery or death) occur. At the end of the period, the consequences of interactions materialize, i.e., T_t susceptible people become infected. Following our network approach, the number of newly infected individuals T_t can be written as follows

$$T_t = \left(m_t^S P_t^c\right)^{\gamma} \left(m_t^S P_t^n\right)^{(1-\gamma)} \tag{4}$$

where γ is the relative weight of infection via consumption. The term $m_t^S P_t^c$ $(m_t^S P_t^n)$ represents the number of newly infected people through consumption (work) activities. Hence, the law of motion of the fraction of susceptible individuals in the economy is given by $m_{t+1}^S = m_t^S - T_t$, or

$$m_{t+1}^S = m_t^S - m_t^S \left(P_t^c\right)^{\gamma} \left(P_t^n\right)^{(1-\gamma)} = m_t^S \left(1 - \left(P_t^c\right)^{\gamma} \left(P_t^n\right)^{(1-\gamma)}\right). \tag{5}$$

In any given period $t+1$, the fraction of infected individuals in the population is given by

$$m_{t+1}^I = (1 - \pi_R - \pi_D) m_t^I + T_t. \tag{6}$$

where, π_R represents the rate at which infected people recover from the disease and π_D is the mortality rate. The laws of motion of the fraction of recovered individuals and number of deaths

in the population are $m^R_{t+1} = m^R_t + \pi_R m^I_t$ and $m^D_{t+1} = m^D_t + \pi_D m^I_t$, respectively. And, finally, total population in period $t+1$ (Pop_{t+1}) equals the total population at period t (Pop_t) minus the number of new deaths. That is, $Pop_{t+1} = Pop_t - \pi_D m^I_t$; with $Pop_0 = 1$.

2.4 Susceptible, Infected, and Recovered Individuals' Problems

In this section, we briefly describe the optimization problem of the different types of agents in the economy, i.e., susceptible (S), infected (I), and recovered (R). Let V^J_t denote the time-t value function of a type-J individual, $J = \{S, I, R\}$. A type-J agent problem is to maximize his utility subject to the following budget constraint:

$$(1 + \mu_{ct})c^J_t = (1 - \mu_{nt})w^J_t n^J_t + \Gamma_t, \tag{7}$$

where μ_{nt} is the Pigouvian tax rate on labor income. Note that this policy instrument is not consider in Eichenbaum et al. (2020).

Susceptible Individuals. The lifetime utility of a susceptible agent is given by

$$U^S_t = u\left(c^S_t, n^S_t\right) + \beta[(1 - \tau_t)U^S_{t+1} + \tau_t U^I_{t+1}], \tag{8}$$

where τ_t is the probability a susceptible agent becomes infected:

$$\tau_t = \frac{T_t}{m^S_t} = \left(P^c_t\right)^{\gamma}\left(P^n_t\right)^{(1-\gamma)}. \tag{9}$$

Equation (9) highlights the fact that a susceptible agent internalizes the fact that she can reduce the probability of getting infected by consuming less and working less.

A susceptible agent's problem is to maximize lifetime utility, equation (8), subject to constraints (7) and (9). The first order conditions with respect to consumption, hours worked and τ_t are,

respectively,

$$u_1(c_t^S, n_t^S) - \lambda_{bt}^S(1+\mu_{ct}) + \lambda_{rt}\gamma\left(\frac{P_t^n}{P_t^c}\right)^{1-\gamma}\frac{\partial P_t^c}{\partial c_t^S} = 0, \tag{10}$$

$$u_2(c_t^S, n_t^s) + \lambda_{bt}^S w_t^S(1-\mu_{nt}) + \lambda_{rt}(1-\gamma)\left(\frac{P_t^c}{P_t^n}\right)^{\gamma}\frac{\partial P_t^n}{\partial n_t^S} = 0, \tag{11}$$

$$\beta(U_{t+1}^I - U_{t+1}^S) - \lambda_{rt} = 0, \tag{12}$$

where λ_{bt}^S and λ_{rt} are the Lagrange multipliers associated with equations (7) and (9), respectively. In a non-epidemic economy, the third term of both equations (10) and (11) would not exist. In our model, those terms are the mechanism with which the agents internalize the risks of becoming infected that they take by adopting a given level of consumption and hours worked. Therefore, equations (10) and (11) represent the trade-off between the utility the agents acquire directly by consuming and indirectly by working and the risks they take of becoming infected by consuming and working. A third term, in this sense, yet with another shape, also appears in Eichenbaum et al. (2020). What differs ours from theirs is that, in this model, the social network is internalized.

Infected and Recovered Individuals. The lifetime utility of an infected agent (U_t^I) and a recovered individual (U_t^R) are, respectively,[2]

$$U_t^I = u\left(c_t^I, n_t^I\right) + \beta\left[\left(1-\pi_R-\pi_D\right)U_{t+1}^I + \beta\pi_R U_{t+1}^R\right], \tag{13}$$

$$U_t^R = u\left(c_t^R, n_t^R\right) + \beta U_{t+1}^R. \tag{14}$$

See Appendix A.1 for complete derivations

Production. We assume that there is a continuum of competitive representative firms of unit measure that produce a single good (Y_t) using labor only, according to the following technology $Y_t = A\left(\sum_J \phi^J N_t^J\right)$, where $N_t^J = m_t^J n_t^J$ and ϕ^J denotes the labor productivity of an individual $J = \{S, I, R\}$. Firm's profit maximization $\Pi_t = A\left(\sum_J \phi^J N_t^J\right) - \sum_J w_t^J N_t^J$ implies the following first order condition $A\phi^J = w_t^J$, for $J = \{S, I, R\}$ in every period t.

[2]The expression for U_t^I embodies a common assumption in macro and health economics that the cost of death is the forgone utility of life.

Government. The government budget constraint is as follows:

$$\mu_{ct}\left(\sum_J m^J c_t^J\right) + \mu_{nt}\left(\sum_J w^J N_t^J\right) = \Gamma_t\left(\sum_J m_t^J\right). \tag{15}$$

Equilibrium. In equilibrium, each agent solves her maximization problem and the government constraint is satisfied in each period. In addition, the goods market and labor market clear:

$$\sum_J m^J c_t^J = Y_t, \tag{16}$$

$$\sum_J m^J n_t^J = N_t. \tag{17}$$

and $c_t^J = C_t^J$, $n_t^J = N_t^J$ for $J = \{S, I, R\}$ and every t. In the appendix, we describe our algorithm for computing the equilibrium.

3 Quantitative Analysis

3.1 Model parameterization

In this subsection we report our choice of parameters. As in the preinfection economy (Section 2.2), we assume that a type-J agent's instantaneous utility is given by $u\left(c_t^J, n_t^J\right) = lnc_t^J - \frac{\theta}{2}(n_t^J)^2$. Table I presents our baseline parameters taken from Eichenbaum et al. (2020) for the SIR-Macro model, as well as our benchmark parameters for the network component of our Network SIR-Macro model. The degree distribution we use in this application is a power-law distribution $D_z = (a-1)z^{-a}$, where the power-law exponent, a, determines how heavy the tail of the distribution is,i.e., how common are nodes with much higher than the mean number of peers. We assume agents have on average five peers, $\langle z \rangle = 5$, with $a = 2.25$ (Arbex et al., 2019).

Table I: Model parameters

Preferences, Technology				SIR Model			Network Component				
(1)	(1)	(1)	(1)	(1)	(1)	(1)	(2)	(2)	(2)	(3)	(4)
β	θ	A	ϕ^I	π_D	π_R	ε	a	$\langle z \rangle$	λ_x	γ	ρ_x
$0.96^{\frac{1}{52}}$	0.001275	39.835	0.80	$\frac{(7\times 0.005)}{18}$	$\frac{7}{18} - \pi_D$	0.001	2.25	5	0.95	0.50	0.085

Note: $x = \{c, n\}$;(1) Eichenbaum et al. (2020); (2) Arbex et al. (2019, 2016); (3) Benchmark value; (4) Calibrated.

Several measures have been taken to contain the infection rate (social isolation and the use of personal protective equipment, for example). Thus, and following this literature, we assume that the transmission of the virus from infected agents (I) to their susceptible peers (S) is commanded by $\lambda_c = \lambda_x = 0.95$ (Arbex et al., 2016). Regarding other network parameters, we are conscious of the considerable uncertainty about the true values of these parameters. As a benchmark, we assume that virus transmission via consumption and labor are equally important to the number of newly infected individuals (T_t). That is, we assume $\gamma = 0.5$. The probability at which each agent contacts her susceptible friends either via consumption ($x = c$) or via work ($x = n$), i.e., ρ_t^x, $x = c, n$, is calibrated such that the share of the initial population that is infected in the Network SIR-Macro model peaks at a level similar to Eichenbaum et al. (2020)'s model. In other words, we adjust the probability ρ_t^x, $x = c, n$, to make the Network SIR-Macro model comparable to the Eichenbaum et al. (2020)'s baseline SIR model with respect to the share of the initial population that is infected. Figure 1 illustrates how this share evolves over time in both baseline models. In Eichenbaum et al. (2020), the share of the initial population that is infected peaks at 5.8 percent in week 33. In our model, this share peaks at 5.84 percent in week 29. We conduct a robustness analysis of our results to using different parameter configurations in subsection 3.3.

3.2 Network SIR Model - Progression of an Epidemic

Figure 2 presents the main model results. It illustrates the impact of heterogeneity in the number of connections on the progression of an epidemic. Recall that an economy where agents have on average five peers, $\langle z \rangle = 5$ (our benchmark case), is equivalent to Eichenbaum et al. (2020)'s baseline SIR model. Compared to the benchmark case ($\langle z \rangle = 5$), if agents have more peers on average (i.e., $\langle z \rangle = 6$) the disease initially spreads significantly faster through more connected individuals, but then the spread slows down and the number of infected approaches zero earlier. This reflects the fact that as the infection progresses, fewer peers remain susceptible and are infected and the share of recovered individuals increase. On the other hand, with fewer connections to facilitate transmission, e.g., $\langle z \rangle = 4$, the disease spreads more slowly and the death toll is smaller.

As in Eichenbaum et al. (2020), the epidemic induces a recession: aggregate consumption

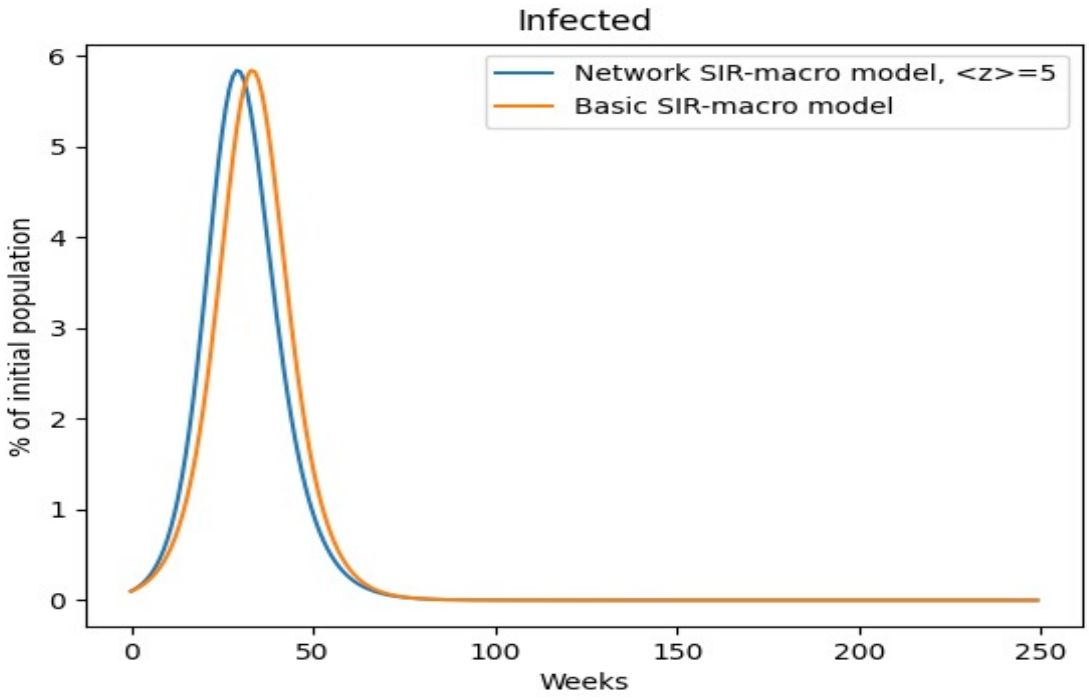

Figure 1: Eichenbaum et al. (2020)'s SIR Model and Network SIR Model

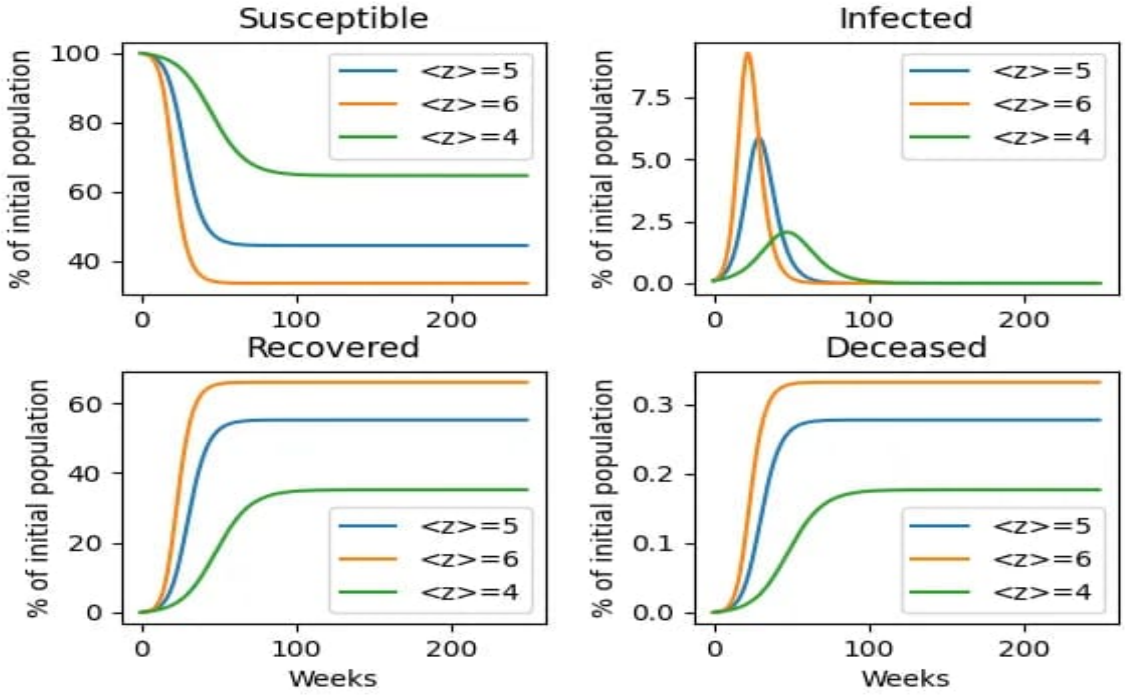

Figure 2: Network SIR Model - Progression of an Epidemic

and hours worked fall (Figure 3). However, the recession is more severe, and occurs sooner, in economies that are more connected (e.g., $\langle z \rangle = 6$). The virus causes more people to be infected earlier in an epidemic and, since infected people are less productive ($\phi^I = 0.80$), they work less hours, earn relatively less income, and, consequently, consume less. The associated negative income effect is stronger and lowers, significantly more, the consumption of those who are infected. In addition, because the share of deceased individuals is higher in more connected economies, the epidemic permanently reduces the size of the work force. This also contributes to the observed fall in aggregate consumption and hours worked in more connected economies. Hence, as Figure 3 illustrates, the network effect amplifies the negative effects of an epidemic.

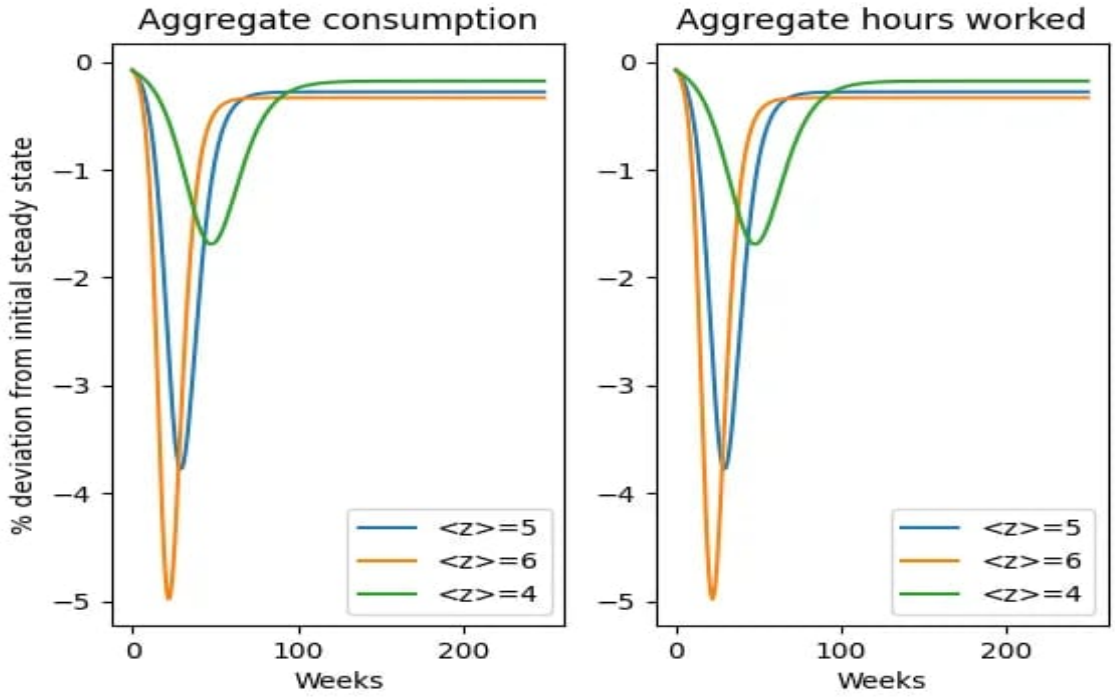

Figure 3: Network SIR Model - Aggregate Consumption (C) and Hours (N)

Notice that in the results presented in Figures 1 and 2, we assumed the same average number of peers $\langle z \rangle$ when individuals engaged in consumption activities and work. However, our model can capture the fact that, for instance, while some individuals may work in large firms (many coworkers; $\langle z_n \rangle$ high), they may consume and interact with fewer people ($\langle z_c \rangle$ low). Next, we present the experiments where we allow for different combinations of $\langle z_c \rangle$ and $\langle z_n \rangle$ to highlight the effects of heterogeneity in the number of (average) peers in consumption and work for the

progression of an epidemic (Figure 4), as well as the aggregate measures of consumption and hours worked (Figure 5).

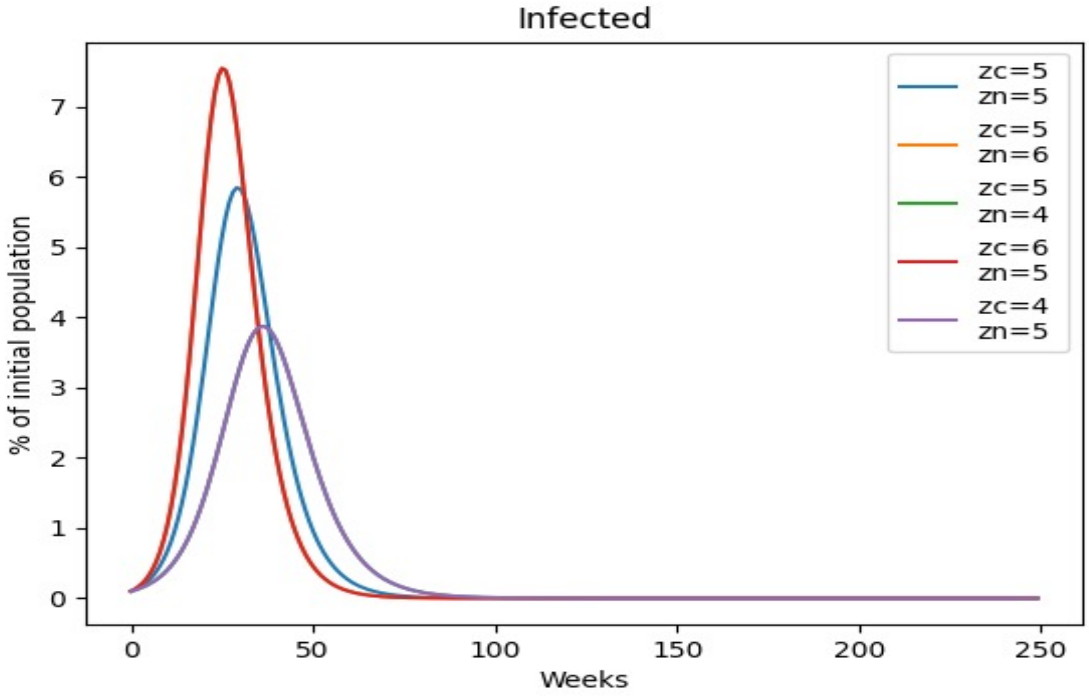

Figure 4: Share of Initial Population Infected - $\langle z_c \rangle$, $\langle z_n \rangle$

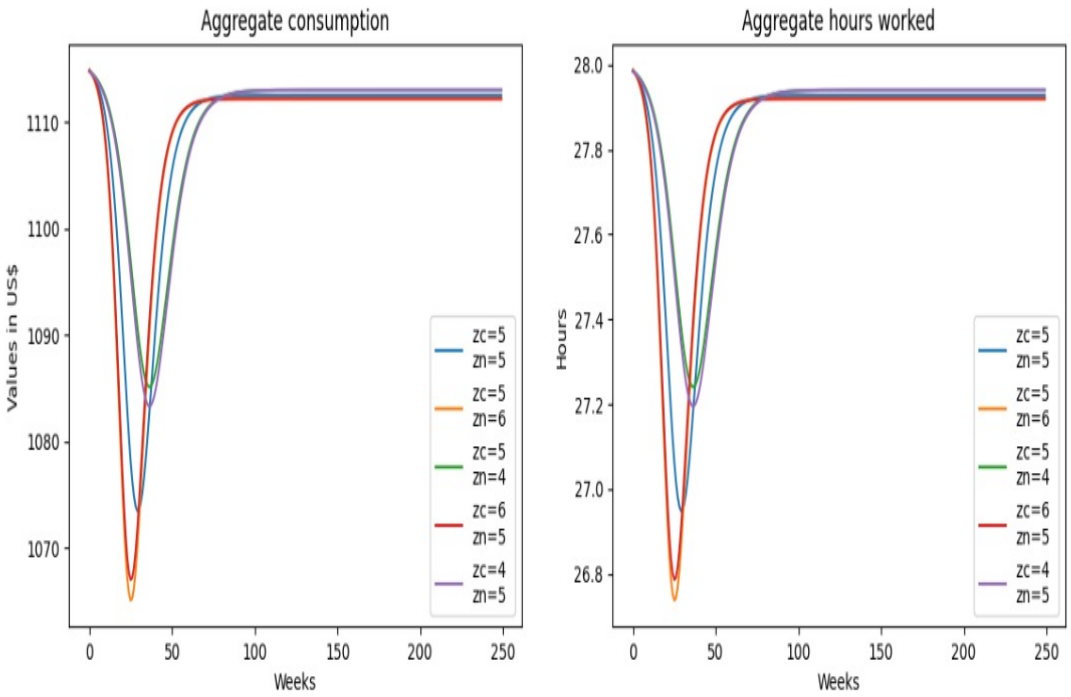

Figure 5: Aggregate Consumption, Hours Worked - $\langle z_c \rangle$, $\langle z_n \rangle$

3.3 Robustness Analysis

Figures 6, 7 and Figure A.3 (Appendix A.3) show how the share of infected people in the population, aggregate consumption and aggregate hours worked are affected by a variety of parameter changes. Although we could perform sensitivity analyses for all parameters, we restrict our attention to those pertinent to social networks. We present and discuss results regarding efficacy of virus transmission (λ), the contact probability (ρ^x, $x = c, n$), and the relative weight of infection via consumption (γ) for our benchmark case $\langle z \rangle = 5$. Figure 6 illustrates that a larger fraction of the population is infected faster the more efficiently the virus is transmitted (i.e., higher λ). In this case ($\lambda_c = \lambda_n = 0.85$), both consumption and hours worked fall more significantly than in the benchmark case ($\lambda_c = \lambda_n = 0.95$). In addition, the results seem to suggest that the distinction between virus transmission efficiency via consumption (λ_c) and work (λ_n) is not particularly relevant. The lower the contact probability $\rho^c = \rho_n$, the lower the share of the population that becomes infected by the virus and the longer it takes to happen. In other words, as the contact probability increases a larger share of the population is infected and this happens sooner. The

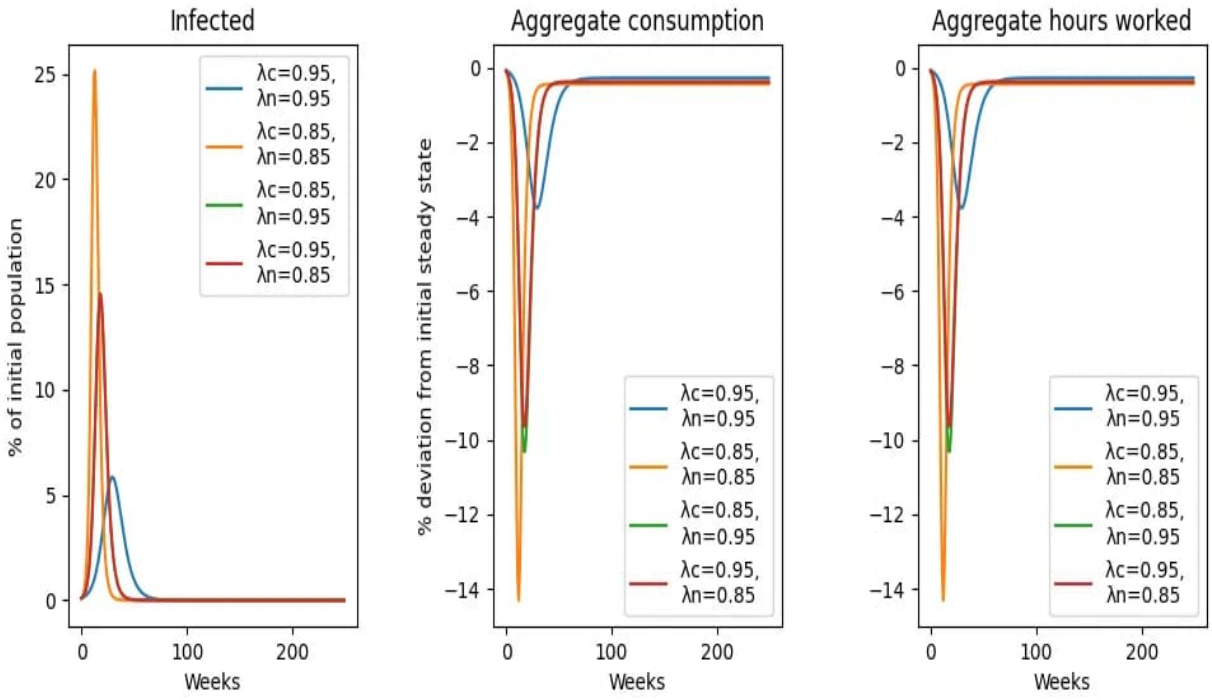

Figure 6: Network SIR Model - Efficacy of Transmission Technology λ_c, λ_x

results displayed in Figure 7 suggest that the share of the population infected reacts in the same fashion either if the consumption contact probability is higher or if the work contact probability is higher. However, the same is not true for the impact of heterogeneity in the contact probabilities on aggregate consumption and hours work. Notice that both aggregate consumption and hours fall more sharply when the contact probability is higher via work (i.e., $\rho_n = 0.20$, $\rho^c = 0.085$ versus $\rho_n = 0.085$, $\rho^c = 0.20$). The intuition is simple. As agents are contacted and infected at work with higher probability, they become sick and are less productive. Their labor income is, hence, lower which, in turn, lower their consumption and consequently the economy's output and consumption (Figure 7). Finally, recall that as a benchmark, we assume that virus transmission via consumption and labor are equally important to the number of newly infected individuals (T_t). That is, we assume $\gamma = 0.5$. Our numerical exercise shows that the results regarding the share of the population infected, aggregate consumption and aggregate hours worked are robust to changes in γ, the relative weight of infection via consumption (Figure A.3, Appendix A.3).

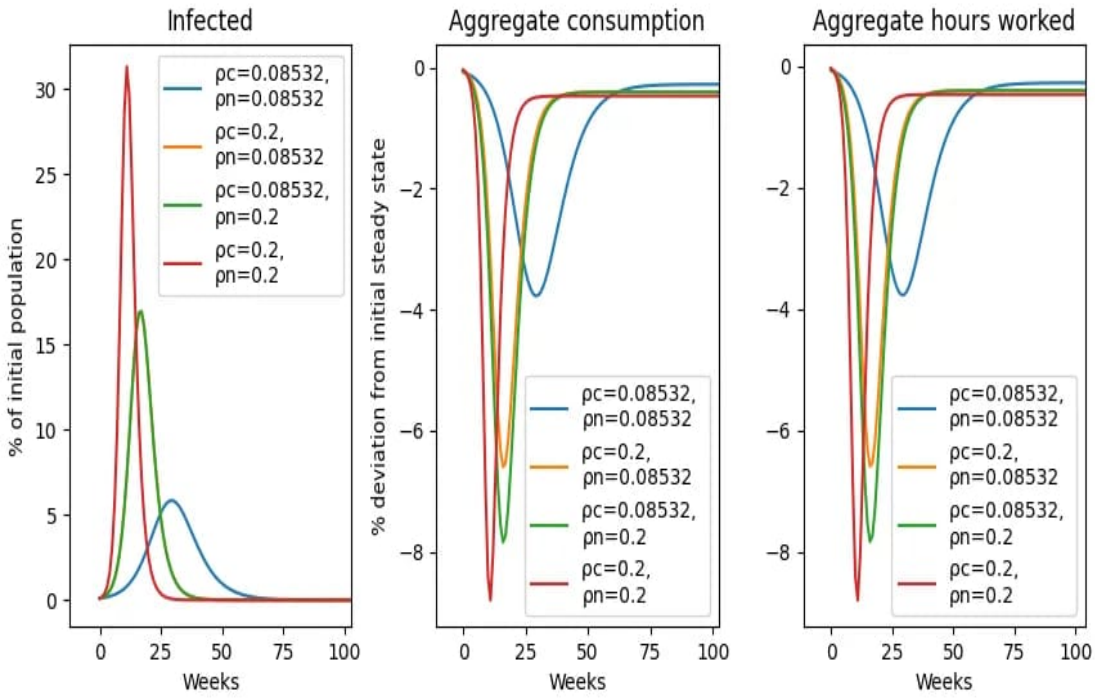

Figure 7: Network SIR Model - Contact Probability ρ^c, ρ^n

4 An application to the Brazilian Economy

4.1 Parameterization

In this section, we present an application of our model to the Brazilian economy. Regarding the parameter values we will highlight only those specific to Brazil; parameters otherwise not mention are assumed to be the same as in the U.S. economy. For parameter that are specific to the Brazilian economy, we use Brazilian data or rely on the Brazilian literature. For parameters that are not specific to the Brazilian economy, we rely on the international literature. The parameter values are shown by Table II.

First, each period of the model corresponds to a week. Moreover, we follow Atkeson (2020) in assuming that it takes 18 days to either recover or to die from the disease. This means that the daily probability to recover or to die, given by $\pi^R + \pi^D$, should equal 1/18. But, because our model is weekly, we will set $\pi^R + \pi^D = 7/18$. We do acknowledge the existence of heterogeneity in life expectancy and efficiency of health systems between different countries. Therefore, we must consider probabilities of dying and recovering from the disease that are adapted to the

Brazilian context. For the value of π^D, we follow Rabelo and Soares (2020), that weighted Brazilian population age groups by the correspondent mortality rate in South Korea. They dropped the population aged more than 70 years, once their job market participation is relatively low, to finally get a (daily) mortality rate of 0,3%. Converting to weekly rate, we have $\pi^D = 7 \times 0.003/18$. π^R is given by: $\pi^R = 7/18 - \pi^D$.

The technological parameters A and θ were chosen to match, at the pre-epidemic steady state, the number of weekly hours worked in Brazil at 2020 (39.1 hours per week) and the Brazilian weekly income *per capita* of 2020 (BRL $1,380.00/4$). For that, we use the average hours worked per week of people aged 14 years old or older and the real average monthly income *per capita*. We obtain the average number of hours worked from SIDRA[3], from IBGE (Brazilian Institute of Geography and Statistics) [4] and the weekly *per capita* income at 2020 from the National Household Sample Survey (PNAD), from IBGE.

Table II: Calibration and description of parameters

Parameter	**Description**	**Value**
π_D	Weekly mortality rate	$(7 \times 0.003)/18$
π_R	Weekly recovery rate	$7/18 - \pi_D$
ε	Initial infected population	0.001
A	Labor augmenting technology	8.82352941
θ	Desutility of labor	0.0006541
β	Weekly discount factor	$0.966^{\frac{1}{52}}$
ϕ^S	Productivity of susceptible people	1
ϕ^I	Productivity of infected people	0.8
ϕ^R	Productivity of recovered people	1
a	Parameter of the *degree distribution* D_z	2.25
λ_c	Inefficacy of infection via consumption	0.95
λ_n	Inefficacy of infection via working	0.95
γ	Relative weight of infection via consumption	0.5

Just like Eichenbaum et al. (2020), we calibrate the value of the parameter that controls the relative productivity of the infected population, ϕ^I, to 0.8. This value is consistent with the idea that symptomatic people do not work and with the hypothesis that 80% of the infected population is asymptomatic, according to the Chine Center for Disease Control and Prevention. Therefore,

[3]IBGE's Automatic Recovery System.
[4]Table 6373.

just like Borelli and Góes (2020), we do not adapt such parameter to the Brazilian context.

In contrast, all the previously calibrated parameters, π^R, π^D, A and θ, reflect the Brazilian characteristics. Also, we assign the value of $\beta = 0.966^{\frac{1}{52}}$ in order to get a value of life of BRL 2.9 million. This value of life is based on recent estimates for Brazil (Ferrari et al. (2019) and Rocha et al. (2019)). For the initial infected population, ε, we consider a fraction 0.001 of the total population. Again, ρ_t^c and ρ_t^n are treated as constants and are calibrated such that the share of the initial population that is infected in the Network SIR-Macro model peaks at a level similar to Eichenbaum et al. (2020)'s model: $\rho_t^c = \rho_t^c = 0.09$. Note that its value is not the same as in the calibration for the USA.

4.2 Results

In general, the dynamics of the pandemic happens the following way: from a unit population, a fraction ε gets infected by the virus at the time 0. The fraction of susceptible people is, therefore, $1 - \varepsilon$. At first, for $\varepsilon = 0.001$, the susceptible population is relatively high. This makes the new weekly infections, given by T_t, relatively high as well, what, thus, increases both the infected population and the new value of T_1.

Such process continues until the number of infected people reaches a peak at some given time, from where the number of new infections stops increasing because of the reduction of the susceptible population. In our numerical exercise, the infected population peaks at the thirtieth week, representing 5.72% of the initial population. Thus, the previous process reverses, and the number of infected people falls as the number of new infections falls. In the end of the pandemic, nearly 64.90% of initial population will eventually have been infected.

At this point, the number of recovered people has reached a significant fraction of the total population, and its growth is, in the absence of treatments and vaccines, the only way of ending the pandemic, which is called the "herd immunity". In our simulation, the long run recovered population represents 54.90% of the total population, while 44.93% remains susceptible. Total deaths represent 0.16% of the initial population. Figure 8 shows this dynamics.

From the macroeconomics perspective, the dynamics of the epidemic induce recessions. The aggregate consumption falls for two reasons. The first one is due to the low productivity of the

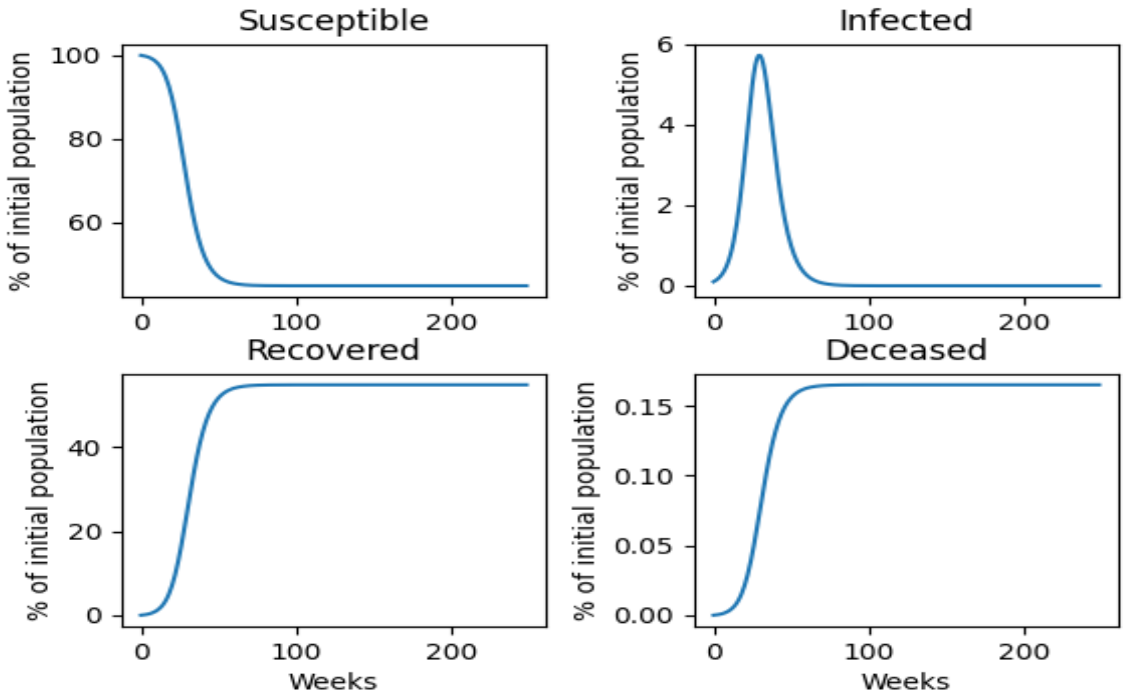

Figure 8: Dynamics of the populations

small fraction of the population that remains infected. The second, and more important, is due to the number of deaths during the pandemic, that, in turn, also leads to a permanent reduction of the workforce.

In this first analysis, we present the results for the competitive equilibrium, where the government does not interfere in the economy to control the evolution of the pandemic. The dynamics of the pandemic is affected only by the decisions of the economic agents, who has the freedom to reduce their own probabilities of infection by reducing consumption and hours worked.

Similar to what Eichenbaum et al. (2020) found, the results point to a scenario that only susceptible people are concerned about reducing the infection rate by consuming and working less. Figure 9 shows this pattern. The recovered people are indifferent to the pandemic, for they can no longer get infected, and, thus, act according to what they would act if there was no pandemic.

On the other hand, the infected people reduce consumption, not to control the pandemic though, but because, given their lower labor productivity, their income is also lower, and, thus, they face a higher budget constraint. They are obligated to consume less than the recovered agent. More precisely, they consume approximately 20% less then their pre-pandemic steady

state consumption, while the recovered agent consumes exactly what they would consume at the pre-pandemic steady state.

However, their hours worked do not differ from the steady state: because they are already infected, they do not have anything to lose by working - similar to the recovered people. But, more precisely, the infected agent's hours worked equals the recovered agent's because the desutility of labor, θ, is the same for all agents. But, say, if we set a higher level of such parameter to the infected agent, then her hours worked would shift down just like her consumption did.

The susceptible agent's behavior on consumption and hours tends to imitate the trajectory of the infected population in its upside down form. As already said, the susceptible agent seeks to avoid infection by reducing contact with other people through consumption and hours worked. As the number of infected people grow, so do grow the probability of becoming infected. Therefore, these agents must cut even more on consumption and hours worked. This process continues until the susceptible agent consumes and works 2.20% less then her steady state levels.

When the infected population falls, the opposite occurs: the probability of becoming infected also falls, and, then, the susceptible agent can gradually increase her consumption and hours worked until she returns to her pre-pandemic steady state level.

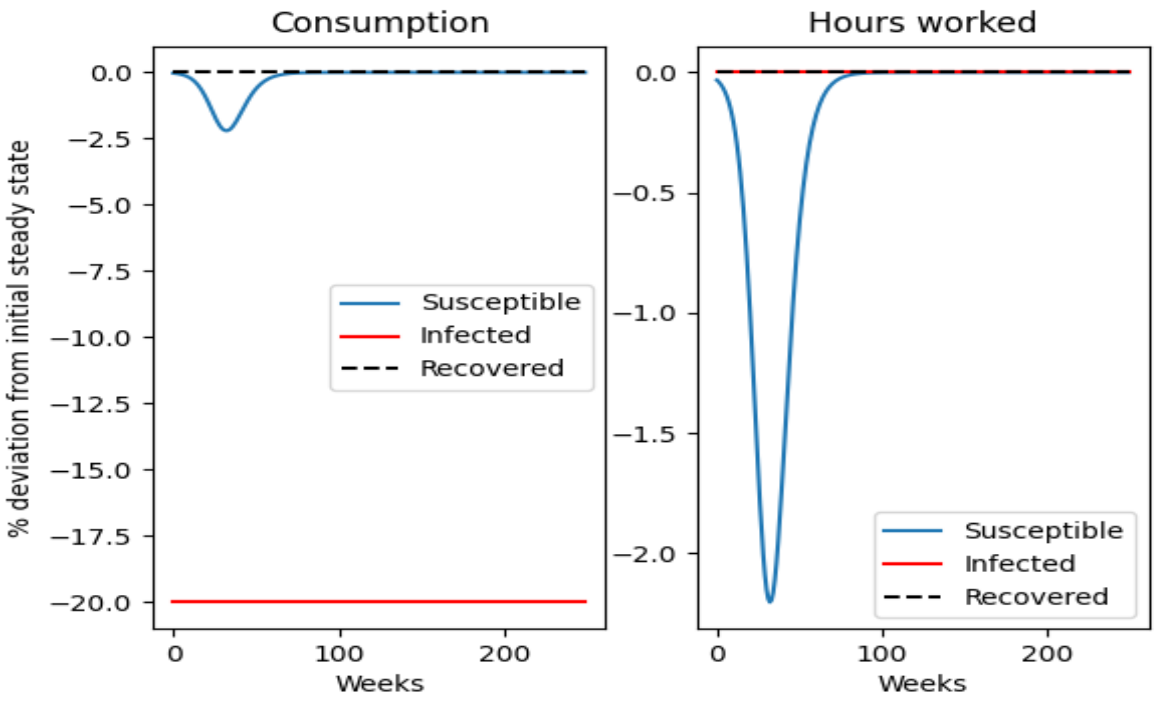

Figure 9: Agents' consumption and hours worked.

4.2.1 Economies with different average number of links

Now we shall look at what happens when we increase the average number of peers of the economy, given by $\langle z \rangle$. We do this by reducing the value of the parameter a. In the baseline calibration, $\langle z \rangle = 5$ corresponds to $a = 2.25$, while $\langle z \rangle = 6$ corresponds to $a = 2.1$, and $\langle z \rangle = 4$ corresponds to $a = 2.6$.

The figures below present the results. Figure 10 shows the dynamics of the populations, while Figure 11 shows the consumption and work trajectory for the susceptible agent alone, because the infected and recovered agents would maintain their behavior constant, just like in Figure 9.

Intuitively, one could expect that more connected economies would produce more infected people and more deaths during a pandemic. And that is confirmed by the results. The populations dynamics, shown by Figure 10, says that more connected economies are associated with more infected people and more deaths. The blue, orange and green lines indicate an economy where the average number of peers equals 5, 6 and 4, respectively.

When $\langle z \rangle = 6$, the infected population reaches the peak seven weeks sooner, at the twenty

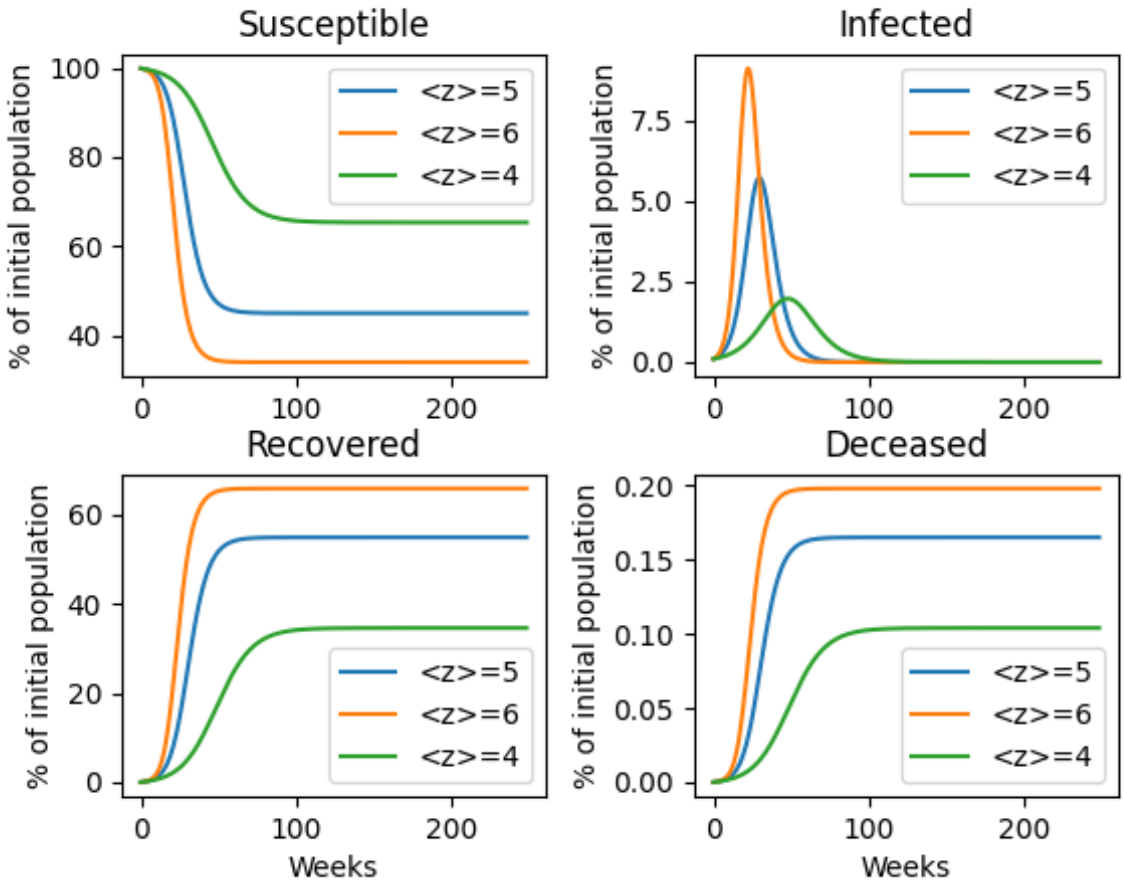

Figure 10: Populations dynamics for different $\langle z \rangle$.

third weak. In that week, infected represent 9.12% of the total population, which is a little growth compared to the baseline calibration. In addition, 67.87% of the total population are recovered in the long run, which is also higher, because more people becomes infected and, thus, recover from the disease. Moreover, 33.93% remain susceptible, which is less than the baseline calibration, and the deaths represent 0.19% of the initial population, which is also a growth.

If we set $\langle z \rangle = 4$, it is the less severe scenario. Infected population peaks twenty weeks later than the baseline calibration: at the fiftieth week, reaching only 1.95% of the total population. In the long run, the recovered population decreases to 34.57%, because the large increase in the number of infected people. Consequently, the susceptible population falls to 65.31%, and total deaths fall to 0.10% of the initial population, as expected.

Intuitively, that is the expected result. Because, on average, the number of peers is relatively

high, more connected societies allow a faster spread of the virus through their social network. That will cause more infections, thus, more deaths, and, consequently, less susceptible and more recovered people.

In the model, the increase of $\langle z \rangle$ is first introduced, at the first period, only in equation (3). Note that the probability a susceptible agent receives the virus from a given peer, given by (2), does not change in the first period with the increase of $\langle z \rangle$.

Analytically, the answer is obvious: both Ω_t^c and Ω_t^n do not depend on the parameter a or $\langle z \rangle$. Intuitively, we must note that, in the first period, the probability a susceptible agent receives the virus from a given peer must not change because there was no time yet for the virus to spread through the social network: the virus is introduced by an external source. The same applies to the probability a susceptible agent of type z receives the virus from at least one peer, given by $p_t^x, x = c, n$.

Differently from the previous equations, equation (3) introduce the effects of the increase of $\langle z \rangle$ right from period 0. Analytically, it is easy to note that both equations integrate the term D_z, which is given by $(a-1)z^{-a}$, and the parameter a appears. The intuition behind it is the following: equation (3) represents the probability the average susceptible agent receives the virus via her network. In this case, there is a crucial difference compared with the previous equations: the average susceptible agent has changed.

The average susceptible person has $\langle z \rangle$ peers. But in the baseline calibration, that number is 5, while in the other calibrations, that number increases to 6 and reduces to 4. Therefore, even at the first period, the average person that has 6 links is more likely to receive the virus through her social network than if she had 5 links. It is true that equation (2) also refers to the average person. However, they do not account for receiving the virus from her entire social network. It accounts only for receiving the virus from a given peer.

Figure 11 shows the trajectories of the susceptible agent consumption and hours worked for different levels of $\langle z \rangle$. We focus only on the susceptible agent because both recovered and infected agents do not change their behavior when we change $\langle z \rangle$, for they are not worried about getting infected. Susceptible people, on the other hand, do care about the number of $\langle z \rangle$, because it will

define the evolution of the pandemic, shown by Figure 10, and, thus, influence the probability of becoming infected.

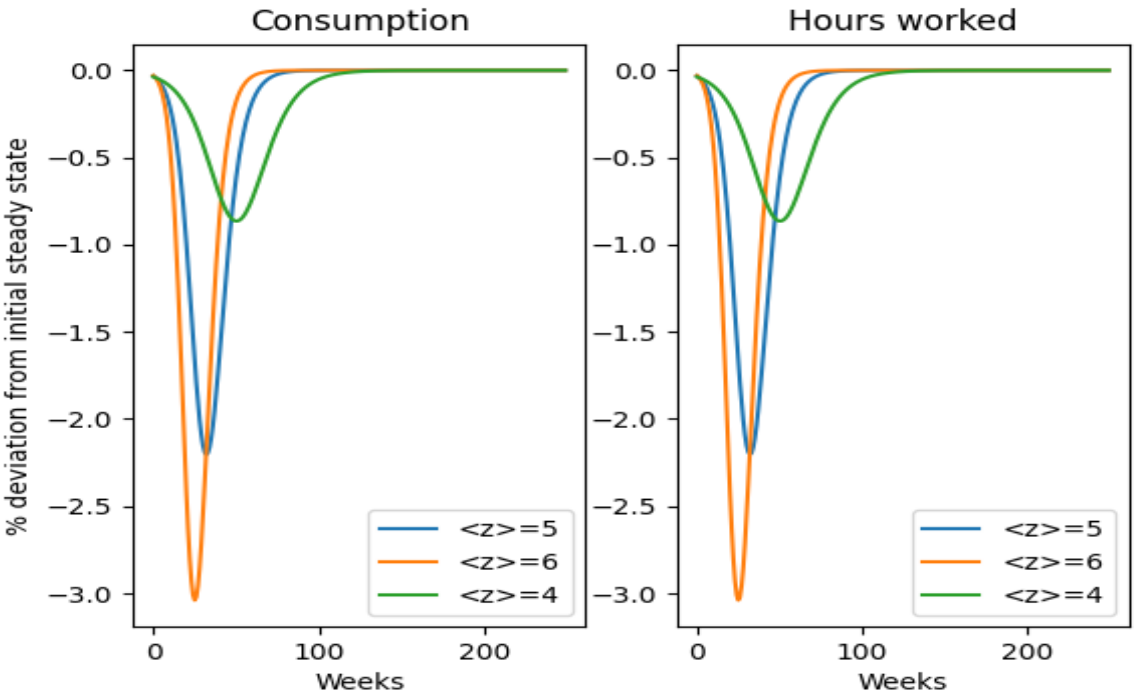

Figure 11: Consumption and hours worked by susceptible agent for different $\langle z \rangle$.

When, on average, people have 5 peers, the susceptible agent cuts less on consumption and work, than when the average number of links is 6 and cuts more on those activities when compared to the scenario where $\langle z \rangle = 4$. At the bottom of the curve, as already said, these agents consume and work approximately 2.20% of their steady state level. When the average number of peers is 6, the agents cut more on their economic activities, until the consumption and the hours worked reach a fall of about 3.03% of the their steady state levels. In an economy where $\langle z \rangle = 4$, it is, again, the less severe scenario: the susceptible agents decrease their consumption only until they consume and work approximately 0.86% less than their steady state levels.

4.3 Robustness

In this subsection, we do robustness check on the only parameter we do not have a sufficiently reliable source, which is γ, the parameter governing the relative weight of infection via consumption. In the baseline, it was set $\gamma = 0.5$.

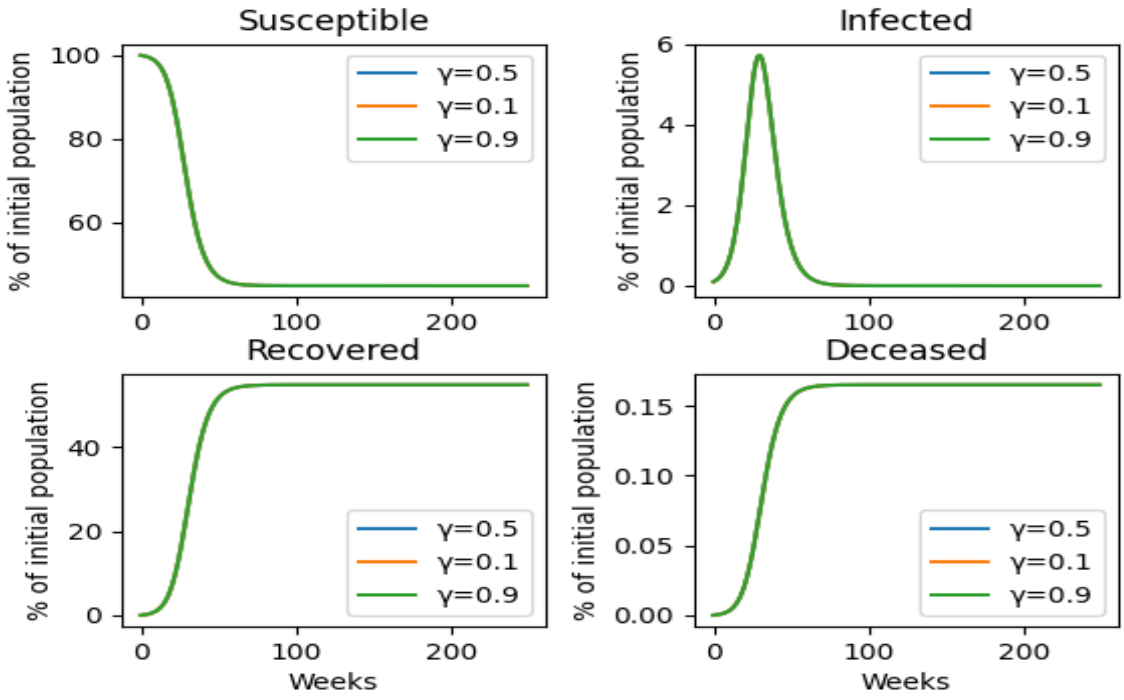

Figure 12: Populations dynamics for different γ.

Figure 12 shows the dynamics of the populations for different values of γ. By running the model with extreme values - 0.1 and 0.9 -, we get the same result as the one of the baseline. The blue line, corresponding to the baseline calibration, was overlapped by the orange one, that represents the scenario where $\gamma = 0.1$, and the orange line was overlapped by the green line, that represents $\gamma = 0.9$. Therefore, we can state that the results will change little if we change the value of γ. Thus, we maintain our guess that $\gamma = 0.5$ without great concern.

Now we analyze the behavior of the consumption and hours worked of each type of agent as γ changes. Figures 13 and 14 show that behavior for the infected and recovered agents.

The same result we found at the populations dynamics is confirmed here: the results do not change with variations of γ. The blue line was overlapped by the orange line, which was also overlapped by the green line. Thus, infected and recovered agents do not change their behavior according to changes in γ. But susceptible agents do change their behavior, as shown by Figure 8.

When $\gamma = 0.1$, the susceptible agent's consumption and hours worked minimum represents a 2.09% fall of their steady state levels. It is higher than the minimum achieved in the baseline calibration, which is a fall of 2.20%.

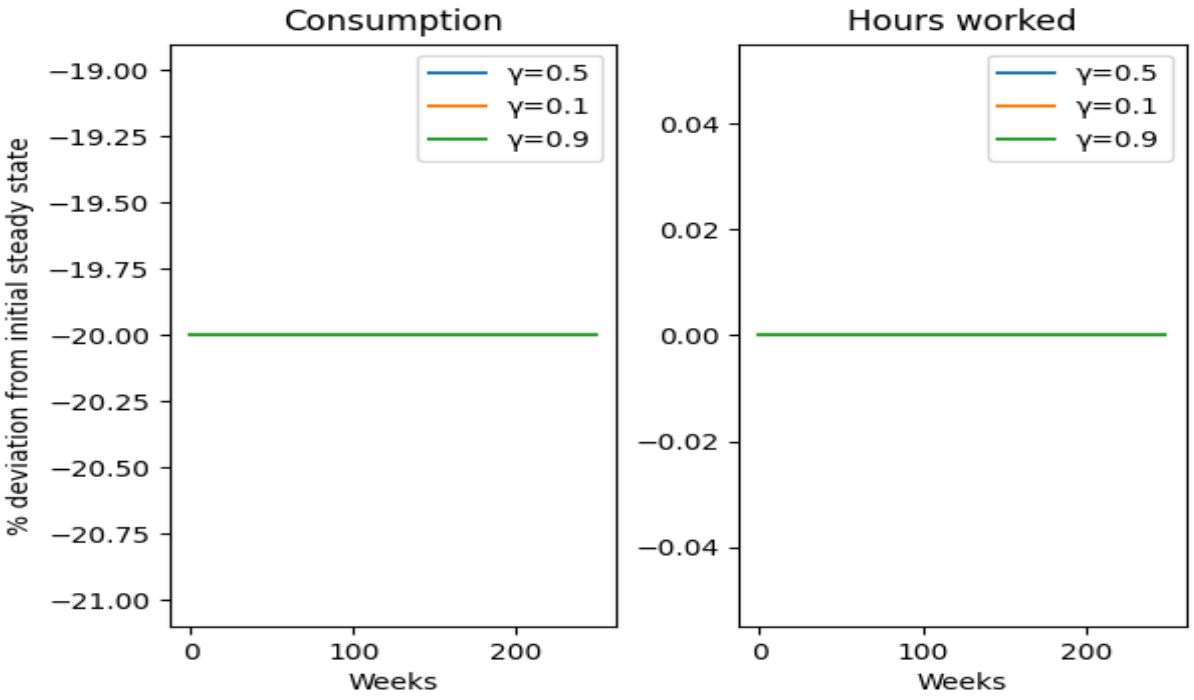

Figure 13: Infected agent's consumption and hours worked for different γ.

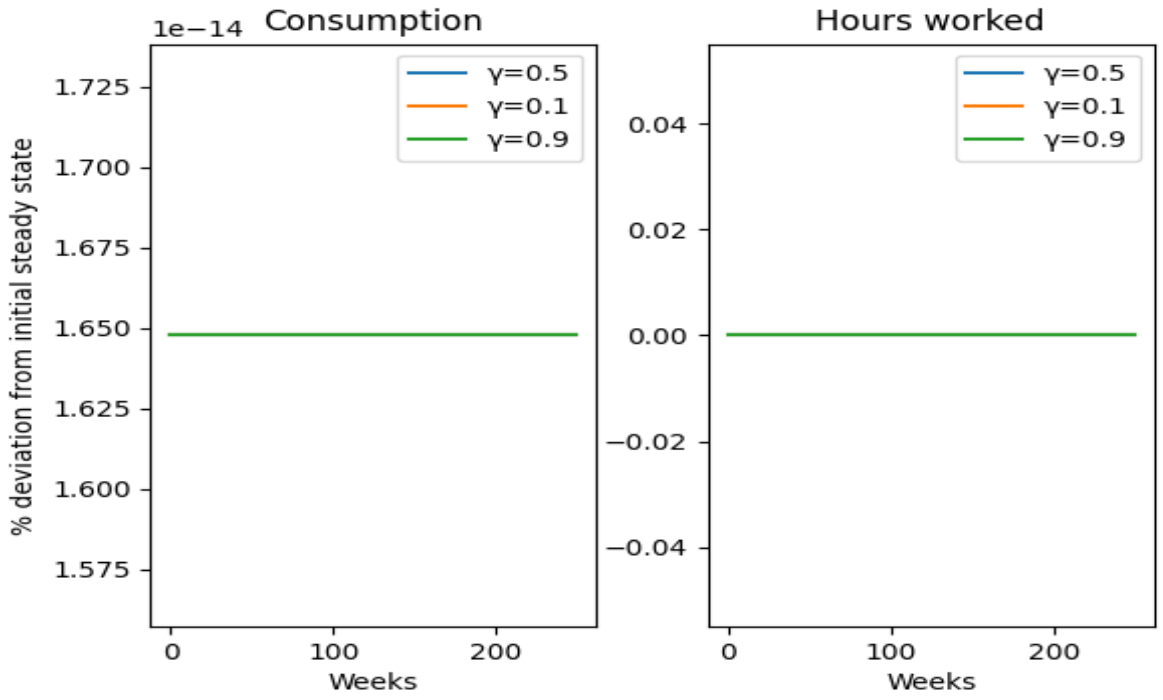

Figure 14: Recovered agent's consumption and hours worked for different γ.

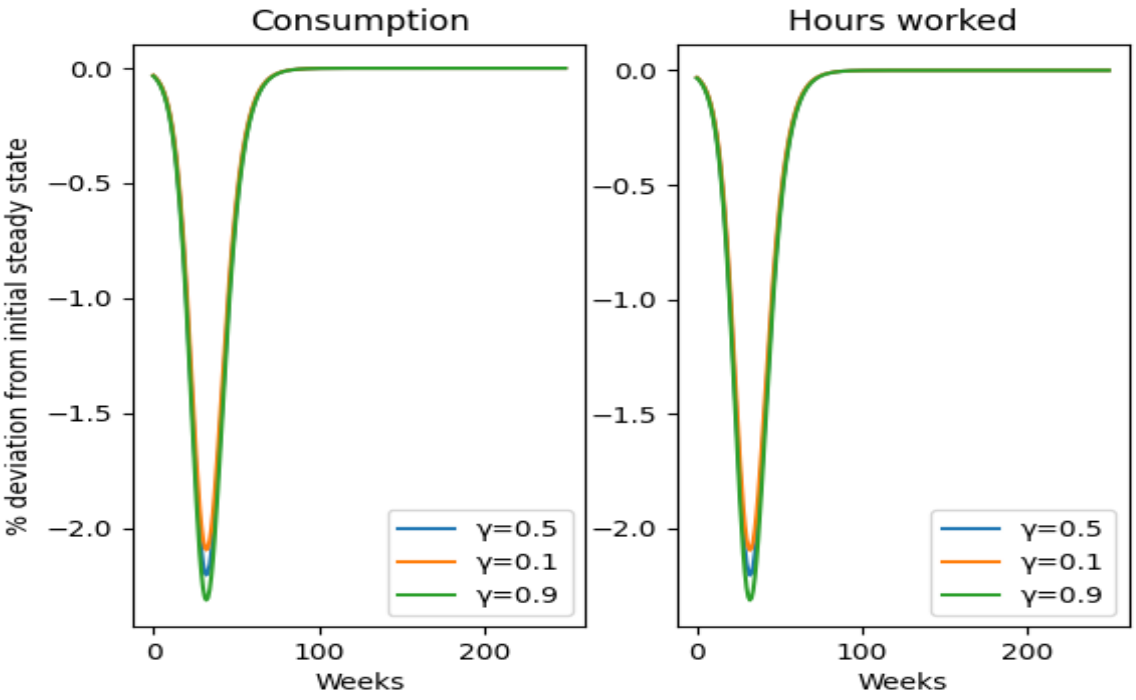

Figure 15: Susceptible agent's consumption and hours worked for different γ.

Although γ is the relative weight of infection via consumption, the higher it is, the lower is the relative weight, because P_t^c, its base (see equation (4)) is between 0 and 1, for it is a probability. Note also that, according to equation (4), 1-γ is the relative weight of infection via work. Now, a higher γ means a higher weight. In this specific case, when we set $\gamma = 0.1$, we are decreasing its value compared to the baseline calibration - $\gamma = 05$ -, and, thus, increasing the relative weight of infection via consumption and decreasing the relative weight of infection via work.

According to our algorithm, the agents first decide how much to work, and, based on such decision, they consume. Because $\gamma = 1$ represents a decline of the relative weight of infection via work, the susceptible agent would like to work more when compared to the baseline calibration. Thus, the susceptible agent's hours worked has the "U" shaped format, because of the pandemic, but it slightly shifts up.

The opposite occurs when we increase γ to 0.9. Because the relative weight of infection via work has increased, the susceptible agent would like to work less compared to the baseline calibration: the "U" shaped trajectory of hours worked shifts down. At its minimum level, the susceptible agents works 2.31% of the steady state hours worked. Based on such trajectory, her consumption

decision is also similar, reaching a 2.31% fall of steady state consumption at its minimum.

Although we find important and intuitive changes on the susceptible agent's decision on consumption and hours worked, changes on the parameter γ are change the main results very little. The trajectories of the populations and the infected and recovered agents' decisions on consumption and hours worked does not change, and the changes found on the susceptible agent's consumption and hours worked are relatively small - about 0.22%. Therefore, we are confident to state our main results with the baseline calibration of $\gamma = 0.5$.

5 Conclusion

In this paper, we analyze the specific effects of the COVID-19 pandemic on the Brazilian economy, given the characteristics of its economy and social network. In addition, we study the sensibility of the dynamics of the pandemic on the social network features. For that, we use a Susceptible-Infected-Recovered (SIR) model adapted to a network environment. In our model, a person with a higher number of links will be more likely to get infected through its network. Therefore, the higher the average number of links in the society, the virus will spread faster, leading to more infected people and more deaths. Recovered people maintain their level of pre-pandemic state steady consumption and hours worked because they no longer can be infected by the disease. Infected people also cannot be infected again by the disease, and thus, they also act as if there was no pandemic, but the difference is that, because these people are less productive, and, thus, consume less than they did at the pre-pandemic steady state. On the other hand, susceptible people, during the course of the pandemic, decrease their consumption and hours worked in order to avoid contact with other people, and, thus, avoid acquiring the disease. With respect to the social network, in more connected economies, the number of infected people is higher. With this, the susceptible agents reduce their consumption and hours worked even more, because the chances of getting infected increase. The opposite is also true: In less connected economies, with less infected people, the susceptible agents' consumption and hours worked, despite reducing because of the presence of infected people, such reduction is quite slighter.

References

Acemoglu, D., V. Chernozhukov, I. Werning, and M. D. Whinston (2021): "Optimal Targeted Lockdowns in a Multigroup SIR Model," *American Economic Review: Insights*, 3, 487–502.

Acemoglu, D., V. Chernozhukov, I. Werning, M. D. Whinston, et al. (2020): *A multi-risk SIR model with optimally targeted lockdown*, vol. 2020, National Bureau of Economic Research Cambridge, MA.

Arbex, M., S. Caetano, and D. OâDea (2016): "The implications of labor market network for business cycles," *Economics Letters*, 144, 37–40.

Arbex, M., D. O'Dea, and D. Wiczer (2019): "Network search: Climbing the job ladder faster," *International Economic Review*, 60, 693–720.

Atkeson, A. (2020): "What will be the economic impact of COVID-19 in the US? Rough estimates of disease scenarios," Tech. rep., National Bureau of Economic Research.

Berger, D. W., K. F. Herkenhoff, and S. Mongey (2020): "An seir infectious disease model with testing and conditional quarantine," Tech. rep., National Bureau of Economic Research.

Bethune, Z. A. and A. Korinek (2020): "Covid-19 infection externalities: Trading off lives vs. livelihoods," Tech. rep., National Bureau of Economic Research.

Borelli, L. and G. S. Góes (2020): "A Macroeconomia das epidemias: heterogeneidade interestadual no Brasil," .

Brinca, P., J. Duarte, and M. Faria-e Castro (2021): "Measuring labor supply and demand shocks during COVID-19," *European Economic Review*, 139, 1–20.

Brodeur, A., D. Gray, A. Islam, and S. Bhuiyan (2021): "A literature review of the economics of COVID-19," *Journal of Economic Surveys*, 35, 1007–1044.

Eichenbaum, M. S., S. Rebelo, and M. Trabandt (2020): "The macroeconomics of epidemics," Tech. rep., National Bureau of Economic Research.

Ferrari, T. K., L. d. A. Dusi, D. A. F. Lopes, and F. M. Pompermayer (2019): "Estimativa do valor da vida estatística e do valor da economia de tempo em viagens nas rodovias brasileiras com a utilização de pesquisa de preferência declarada," .

Gopinath, G. (2020): "The great lockdown: Worst economic downturn since the great depression," *IMF blog*, 14, 2020.

Kermack, W. O. and A. G. McKendrick (1927): "A contribution to the mathematical theory of epidemics," *Proceedings of the royal society of london. Series A, Containing papers of a mathematical and physical character*, 115, 700–721.

Rabelo, M. and J. Soares (2020): "The Macroeconomics of Epidemics: results for Brazil," Tech. rep., Working paper.

Rocha, G., R. L. de Morais, and L. Klug (2019): "O Custo econômico da poluição do ar: estimativa de valor da vida estatística para o Brasil," Tech. rep., Texto para Discussão.

A.1 Theoretical Results

Infected and Recovered Individuals. The value function of an infected agent is

$$V_t^I = \max_{c_t^I, n_t^I} \{u\left(c_t^I, n_t^I\right) + \beta\left[\left(1 - \pi_R - \pi_D\right) V_{t+1}^I + \beta \pi_R V_{t+1}^R\right]\}. \tag{18}$$

The first order conditions with respect to consumption and hours worked of an infected individual are, respectively,

$$u_1(c_t^I, n_t^I) - \lambda_{bt}^I(1 + \mu_{ct}) = 0, \tag{19}$$

$$u_2(c_t^I, n_t^I) + \lambda_{bt}^I w_t^I(1 - \mu_{nt}) = 0, \tag{20}$$

The value function of an recovered agent is

$$V_t^R = \max_{c_t^R, n_t^R} \{u\left(c_t^R, n_t^R\right) + \beta V_{t+1}^R\}. \tag{21}$$

The first order conditions with respect to consumption and hours worked are, respectively,

$$u_1(c_t^R, n_t^R) - \lambda_{bt}^R(1 + \mu_{ct}) = 0, \tag{22}$$

$$u_2(c_t^R, n_t^R) + \lambda_{bt}^R w_t^R(1 - \mu_{nt}) = 0, \tag{23}$$

where λ_{bt}^R is the Lagrange multiplier associated with constraint (7).

A.2 Heterogeneity Number of Connections C and H

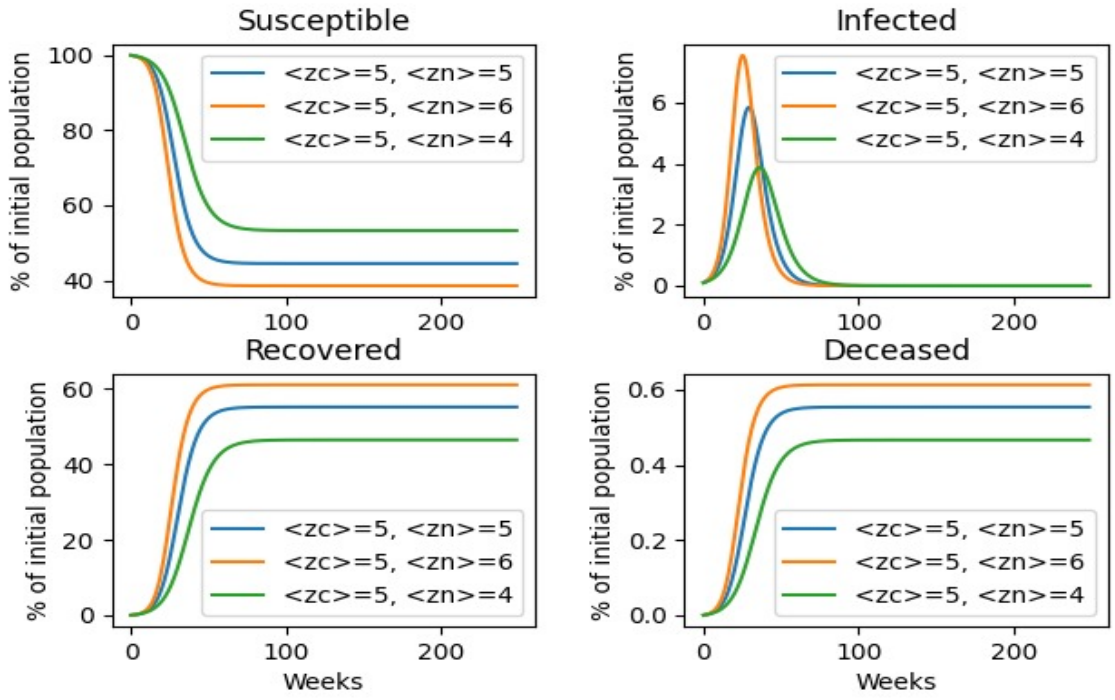

Figure A.1: Network SIR Model - Progression of an Epidemic - $\langle z_c \rangle = 5$, $\langle z_n \rangle$

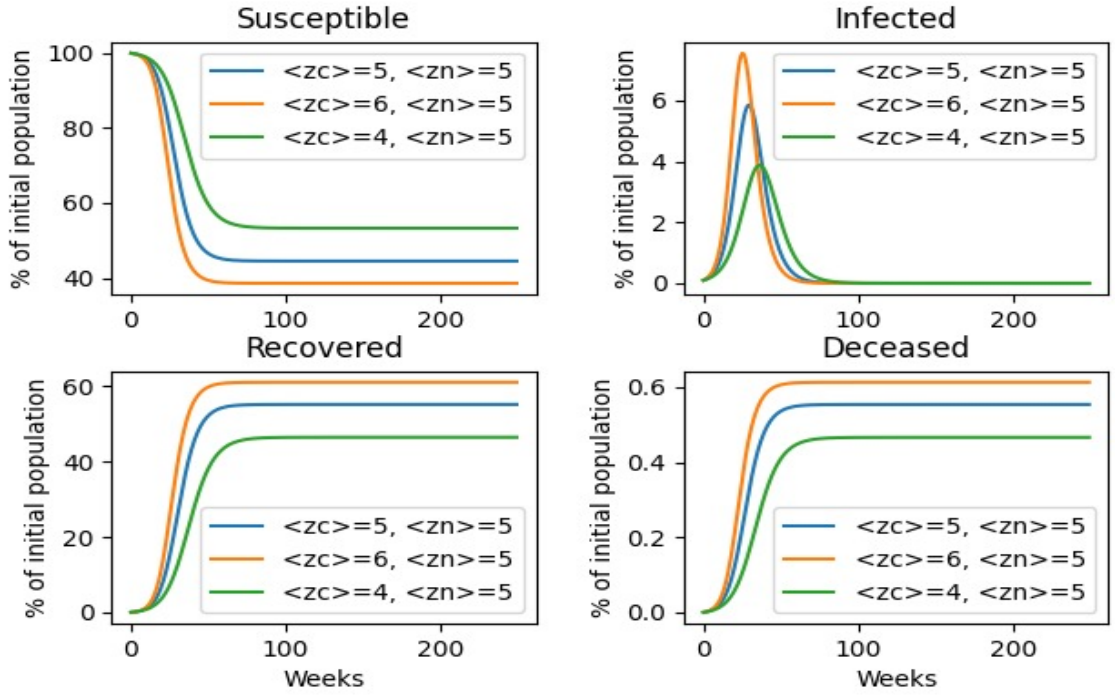

Figure A.2: Network SIR Model - Progression of an Epidemic - $\langle z_c \rangle$, $\langle z_n \rangle = 5$

A.3 Robustness Analysis - Additional Results

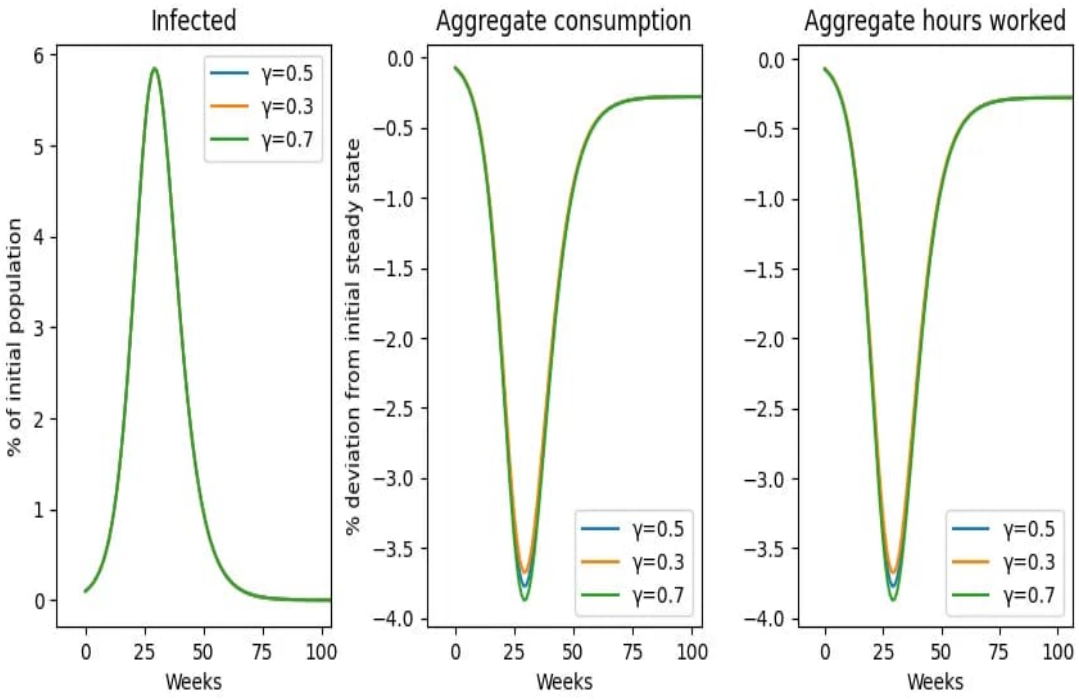

Figure A.3: Network SIR Model - Relative weight of infection via consumption γ

A.4 Algorithm for computing the equilibrium

The algorithm used to compute the equilibrium is similar to the one that was used by Eichenbaum et al. (2020). The difference is that we adjust for the network environment.

For a given sequence of containment rates, $\{\mu_{ct}\}_{t=0}^{H-1}$, for some large horizon, H, guess the sequences for $\left\{n_t^S, n_t^I, n_t^R\right\}_{t=0}^{H-1}$. Similarly, I solve the model for $H = 250$ weeks. Compute the sequence of the remaining unknowns variables in each of the following equilibrium equations:

$$\theta n_t^R = A\lambda_{bt}^R(1-\mu_{nt}),$$
$$\left(c_t^R\right)^{-1} = (1+\mu_{ct})\,\lambda_{bt}^R,$$
$$u\left(c_t^R, n_t^R\right) = lnc_t^R - \frac{\theta}{2}(n_t^R)^2,$$
$$(1+\mu_{ct})\,c_t^R = (1-\mu_{nt})An_t^R + \Gamma_t,$$
$$\theta n_t^I = \phi^I(1-\mu_{nt})A\lambda_{bt}^I,$$
$$\left(c_t^R\right)^{-1} = (1+\mu_{ct})\,\lambda_{bt}^I,$$
$$u\left(c_t^I, n_t^I\right) = lnc_t^I - \frac{\theta}{2}(n_t^I)^2,$$
$$(1+\mu_{ct})\,c_t^S = (1-\mu_{nt})An_t^S + \Gamma_t,$$
$$u\left(c_t^S, n_t^S\right) = lnc_t^S - \frac{\theta}{2}(n_t^S)^2,$$

$$D_z = (a-1)z^{-a},$$
$$\rho_t^c = m_t^s,$$
$$\rho_t^n = m_t^s,$$
$$\Omega_t^c = \rho_t^c \varphi(c_t^I, c_t^S) m_t^I,$$
$$\Omega_t^n = \rho_t^n \varphi(n_t^I, n_t^S) m_t^I,$$
$$p_t^n = 1 - (1 - \Omega_t^c)^z,$$
$$p_t^n = 1 - (1 - \Omega_t^n)^z,$$
$$P_t^c = \int_{z=1}^{\infty} p_t^c D_z dz = (a-1) \int_{z=1}^{\infty} \left[1 - (1-\Omega_t^c)^z\right] z^{-a} dz,$$
$$P_t^n = \int_{z=1}^{\infty} p_t^n D_z dz = (a-1) \int_{z=1}^{\infty} \left[1 - (1-\Omega_t^n)^z\right] z^{-a} dz.$$

Given initial values for Pop_0, S_0, I_0, R_0 and D_0, iterate forward using the following six equations for $t = 0, ..., H-1$:

$$T_t = m_t^S \left(P_t^c\right)^{\gamma} \left(P_t^n\right)^{(1-\gamma)},$$
$$Pop_{t+1} = Pop_t - \pi_D m_t^I,$$
$$m_{t+1}^S = m_t^S - T_t,$$
$$m_{t+1}^I = (1 - \pi_R - \pi_D) m_t^I + T_t,$$
$$m_{t+1}^R = m_t^R + \pi_R m_t^I,$$
$$m_{t+1}^D = m_t^D + \pi_D m_t^I.$$

Iterate backwards from the post-epidemic steady-state value of V_t^S, V_t^I and V_t^R:

$$V_t^R = \max_{c_t^R, n_t^R} \left\{ u\left(c_t^R, n_t^R\right) + \beta V_{t+1}^R \right\},$$
$$V_t^I = \max_{c_t^I, n_t^I} \left\{ u\left(c_t^I, n_t^I\right) + \beta \left[\left(1 - \pi_R - \pi_D\right) V_{t+1}^I + \beta \pi_R V_{t+1}^R \right] \right\},$$
$$\tau_t = \frac{T_t}{m_t^S} = \left(P_t^c\right)^{\gamma} \left(P_t^n\right)^{(1-\gamma)},$$
$$V_t^S = \max_{c_t^S, n_t^S, \tau_t^S} \left\{ u\left(c_t^S, n_t^S\right) + \beta [(1-\tau_t) V_{t+1}^S + \tau_t V_{t+1}^I] \right\}.$$

Calculate the sequence of the remaining unknowns in the following equations:

$$\beta(V_{t+1}^I - V_{t+1}^S) - \lambda_{rt} = 0,$$
$$\left(c_t^S\right)^{-1} - \lambda_{bt}^S (1 + \mu_{ct}) - \lambda_{rt} \gamma \left(\frac{P_t^n}{P_t^c}\right)^{1-\gamma} \frac{\rho_t^c m_t^I \left(1 - \lambda_c\right) m_t^S}{\left(m_t^S c_t^S + m_t^I c_t^I\right)^{\lambda_c}} \int_{z=1}^{\infty} (1 - \Omega_t^c)^{z-1} z^{1-a} dz = 0,$$
$$\left(1 + \mu_{ct}\right) c_t^I = A n_t^I + \Gamma_t,$$
$$m_t^S c_t^S + m_t^I c_t^I + m_t^R c_t^R = A N_t,$$

$$-\theta n_t^S + (1-\mu_{nt})\lambda_{bt}^S w_t^S - \lambda_{rt}(1-\gamma)\left(\frac{P_t^c}{P_t^n}\right)^{\gamma}\frac{\rho_t^n m_t^I\left(1-\lambda_n\right)m_t^S}{(m_t^S n_t^S + m_t^I n_t^I)^{\lambda_n}}\int_{z=1}^{\infty}(1-\Omega_t^n)^{z-1}z^{1-a}dz = 0.$$

A.5 Derivation of susceptible agent's maximization

The susceptible agent seeks to maximize the following function:

$$\max_{c_t^S, n_t^S, \tau_t} V_0^S + \sum_{t=0}^{H-1}\left\{\lambda_{bt}^S\left[(1+\mu_{ct})c_t^S - w_t^S(1+\mu_{ct})n_t^S - \Gamma_t\right] - \lambda_{rt}\left[\tau_t - \left(P_t^c\right)^{\gamma}\left(P_t^n\right)^{(1-\gamma)}\right]\right\}.$$

The first order conditions for c_t^S and n_t^S are given by (15) and (16), respectively. Calculating $\frac{\partial P_t^c}{\partial c_t^S}$:

$$\frac{\partial P_t^c}{\partial c_t^S} = \frac{\partial \int_{z=1}^{\infty} p_t^c D_z dz}{\partial c_t^S}.$$

D_z is given by $(a-1)z^{-a}$. Thus, and according to (3):

$$P_t^c = \int_{z=1}^{\infty}\left[1-(1-\Omega_t^c)^z\right](a-1)z^{-a}dz,$$

$$P_t^c = (a-1)\left[\int_{z=1}^{\infty} z^{-a}dz - \int_{z=1}^{\infty}(1-\Omega_t^c)^z z^{-a}dz\right].$$

Therefore:

$$\frac{\partial P_t^c}{\partial c_t^S} = (1-a)\frac{\partial \int_{z=1}^{\infty}(1-\Omega_t^c)^z z^{-a}dz}{\partial c_t^S},$$

$$\frac{\partial P_t^c}{\partial c_t^S} = (a-1)\int_{z=1}^{\infty}(1-\Omega_t^c)^{z-1}z^{1-a}\left(\frac{\partial \Omega_t^c}{\partial c_t^S}\right)dz.$$

Solving $\frac{\partial \Omega_t^c}{\partial c_t^S}$ separately:

$$\frac{\partial \Omega_t^c}{\partial c_t^S} = \frac{\partial\left[\rho_t^c(m_t^S c_t^S + m_t^I c_t^I)^{1-\lambda_c} m_t^I\right]}{\partial c_t^S},$$

$$\frac{\partial \Omega_t^c}{\partial c_t^S} = \rho_t^c m_t^I \frac{\partial(m_t^S c_t^S + m_t^I c_t^I)^{1-\lambda_c}}{\partial c_t^S},$$

$$\frac{\partial \Omega_t^c}{\partial c_t^S} = \frac{\rho_t^c m_t^I\left(1-\lambda_c\right)m_t^S}{(m_t^S c_t^S + m_t^I c_t^I)^{\lambda_c}}.$$

Therefore:

$$\frac{\partial P_t^c}{\partial c_t^S} = \frac{(a-1)\rho_t^c m_t^I\left(1-\lambda_c\right)m_t^S}{(m_t^S c_t^S + m_t^I c_t^I)^{\lambda_c}}\int_{z=1}^{\infty}(1-\Omega_t^c)^{z-1}z^{1-a}dz.$$

Similarly, doing the same steps:

$$\frac{\partial P_t^n}{\partial n_t^S} = \frac{(a-1)\rho_t^n m_t^I \left(1-\lambda_n\right) m_t^S}{(m_t^S n_t^S + m_t^I n_t^I)^{\lambda_n}} \int_{z=1}^{\infty} (1-\Omega_t^n)^{z-1} z^{1-a} dz.$$